

# Theory of Main Resonances in Directly Modulated Diode Lasers

Catalina Mayol, Raúl Toral, Claudio R. Mirasso, Sergei I. Turovets, and Luis Pesquera

**Abstract**—Domains of existence of the main resonances in directly modulated semiconductor lasers are obtained by application of quasi-conservative theory. The predictions are compared with numerical results coming from a direct integration of the model equations and with experimental observations reported by other groups. In both cases we find a qualitative good agreement. We consider a model that contains explicitly the gain saturation and spontaneous emission terms. We find that the spontaneous emission strongly modifies the qualitative behavior of the instabilities boundaries, while the gain saturation leads to a simple quantitative shift of boundaries.

We also find that modulation of the pump or loss produce equivalent results if the respective modulation amplitudes are conveniently rescaled.

**Index Terms**—Diode lasers, loss modulation, main resonances, pump modulation.

## I. INTRODUCTION

HIGH-SPEED modulation of diode lasers is an important area of study due to the possible applications of these systems. Laser diodes in such circumstances clearly exhibit various kinds of nonlinear behavior, i.e., harmonic distortion, multi-pulse response on the time scale of one modulation period, period doubling, amplitude and/or pulse position bistability, and chaos [1]. Usually, these complicated dynamical phenomena are considered as harmful to practical applications and should be avoided. Nevertheless, there have been some experimental demonstrations of feasibility of using a resonance period doubling regime and pulse position bistability for realizing high-speed optical logic elements [2].

Large capacity information transmission and ultrafast optical processing systems [3], [4], [33] are representative of the possible applications of these systems. Recently, a great deal of interest has been generated by the potential to use lasers running in

a chaotic regime as the carriers of information in secure chaotic communication schemes [5]. In addition to the optical feedback and saturable absorption effects, chaos in laser diodes induced by modulation in the pump current is another option for building transmitters for encoded optical communications.

Before Liu and Ngai [3] succeeded in observing chaos on a 1.55- $\mu\text{m}$  InGaAsP DFB bulk laser, followed by the report of a similar observation in 1.55- $\mu\text{m}$  MQW lasers [6], there had been some controversy in earlier theoretical predictions [7] and experimental results [8], [9]. Specifically, chaotic and high periodic regimes had not been experimentally observed in contrast to numerical predictions based on the rate equations. It is well known [10] that the gain saturation factor contributes to the damping of relaxation oscillations and might be the reason for eliminating chaos. The presence of spontaneous emission in the cavity and the Auger recombination factor have also been numerically examined as being one cause of the suppression of chaos [11]. The importance of noise terms is again under consideration at this moment [12]. Now it is largely accepted that a single-mode laser diode with relatively small gain saturation and spontaneous emission parameters might undergo a period doubling route to chaos under current modulation. From the analytical side, such an impact of these parameters was explained in the framework of the small signal analysis showing an increase of the system damping with increase of the mentioned parameters [13]. In addition, Hori *et al.* [14] suggested that, in the large signal-modulation regime, the spontaneous emission term, besides contributing into a linear damping of the system, leads to an additional nonlinear damping. This effect would change the representation of the Toda oscillator potential topology for the laser and would be also responsible for suppression of chaos. Nevertheless, specific mechanisms of these effects in the large signal regime are not yet fully understood. To the best of our knowledge, a detailed study of the role of spontaneous emission and gain saturation on nonlinear dynamics in the large signal regime is still lacking even in the framework of the simple rate equation model.

In the present work, we have mainly undertaken analytical calculations in the framework of the single mode rate equation model with the aim of clarifying the parameter domains of the basic instabilities involved and to relate them to the reported experiments with 1.55- $\mu\text{m}$  InGaAs DFB lasers [3]. We will restrict ourselves to the study of main resonances since little attention has been paid to them in previous works. Let us take as a response variable the maximum intensity in the optical-power output. As a main resonance, we understand the maximum response of the system to the external perturbation when the modulation frequency of the external perturbation is

Manuscript received March 2, 2001; revised October 30, 2001. This work was supported by DGES (Spain) under Projects PB97-0141-C02-01, BMF2000-1108, and TIC99-0645-C55-02. The work of S. I. Turovets was supported by a fellowship from MEC, Spain.

C. Mayol and R. Toral are with the Departament de Física, Universitat de les Illes Balears, E-07071 Palma de Mallorca, Spain, and also with the Instituto Mediterráneo de Estudios Avanzados (IMEDEA, UIB-CSIC), E-07071 Palma de Mallorca, Spain (e-mail: cati@imedea.uib.es).

C. R. Mirasso is with the Departament de Física, Universitat de les Illes Balears, E-07071 Palma de Mallorca, Spain (e-mail: claudio@imedea.uib.es).

S. I. Turovets was with the Instituto de Física de Cantabria (CSIC), Universidad de Cantabria, Facultad de Ciencias Avda, E-39005 Santander, Spain. He is now with Siros Technologies, Inc., San Jose, CA 95134 USA.

L. Pesquera is with the Instituto de Física de Cantabria (CSIC), Universidad de Cantabria, Facultad de Ciencias Avda, E-39005 Santander, Spain.

Publisher Item Identifier S 0018-9197(02)01758-X.

varied. Although main resonances were considered for conventional class  $B$  lasers<sup>1</sup> theoretically and numerically [15]–[19] and also experimentally [20], [21], the impact of large gain saturation and spontaneous emission terms, which are typical for diode lasers, is not yet fully understood, and the aim of our work is to go deeper into this context.

By using the asymptotic quasiconservative theory (QCT) [15], [22] with an appropriate Lyapunov potential<sup>2</sup> describing the laser dynamics [23], we have computed the domains of existence for the resonance  $nT$  periodic responses in arbitrarily large amplitude modulated laser diodes. For this particular kind of nonlinearity, these resonant curves are associated to the so-called primary saddle-node bifurcations<sup>3</sup> and are often confused in experiments with the multiperiodic windows in chaos. When considering gain saturation and spontaneous emission terms on the dynamics, we find that, besides increasing the damping of relaxation oscillations, these parameters change the topology of the Lyapunov potential, increasing the thresholds of instabilities in the system. The theory is substantiated by numerical results. The estimations for primary saddle-node bifurcations in strongly modulated laser diodes create the basis for a systematic search for *a priori* wanted regimes in simulations or experiment and also naturally explain pulse position multistability [2], [20].

The paper is organized as follows. In Section II, we describe qualitatively the response obtained for a laser diode, as described by a single-mode rate equation model, in the presence of pump modulation. In Section III, the equations for the laser are rewritten as a relaxational dynamics with a Lyapunov function and modulation terms. The QCT is used to obtain relations that allow the calculation of the primary saddle-node bifurcations, both for the case of modulation in the pump or in the losses. In Section IV, the theoretical estimates are compared with numerical results coming from a direct integration of the model equations. The effects of gain saturation and spontaneous emission terms in these bifurcations are explored in detail. In Section V, we compare our results to previous experimental works reported by other groups. Finally, in Section VI, we summarize the main results.

## II. DYNAMICAL BEHAVIOR

The dynamics of a single mode semiconductor laser can be described in the simplest way by two evolution equations: one for the slowly varying complex amplitude of the electric field inside the laser cavity,  $E$ , and the other for the carriers number  $N$  (or electron-hole pairs) [4], [33]. We consider the electric

<sup>1</sup>For class  $B$  lasers, of which semiconductor lasers are an example, the polarization decays toward the steady state much faster than the field and carrier number, and it can be adiabatically eliminated. They are then described by just two rate equations.

<sup>2</sup>The Lyapunov function, also called Lyapunov potential, is a potential description of the system and it is, in some cases, useful to describe its dynamics (in this case the laser). The usefulness of Lyapunov functions lies on the fact that they allow an easy determination of the fixed points of a dynamical (deterministic) system as the extrema of the Lyapunov function, as well as determining the stability of these fixed points.

<sup>3</sup>In a saddle-node bifurcation, two fixed points of the dynamical system collide in the phase space when some parameters are varied. The saddle-node condition is given when one of the eigenvalues of the Jacobian of the transformation is zero.

TABLE I  
DEFINITIONS AND TYPICAL VALUES OF THE PARAMETERS FOR SEMICONDUCTOR LASERS

PARAMETERS	VALUES
Injection current (bias current) $J$	> threshold
Cavity decay rate $\gamma$	$0.5 \text{ ps}^{-1}$
Carrier decay rate $\gamma_N$	$10^{-3} \text{ ps}^{-1}$
Number of carriers at transparency $N_o$	$1.5 \times 10^8$
Differential gain parameter $g_N$	$1.5 \times 10^{-8} \text{ ps}^{-1}$
Gain saturation parameter $\epsilon$	$10^{-8} - 10^{-7}$
Spontaneous emission rate $\beta$	$10^{-11} - 10^{-8} \text{ ps}^{-1}$
Electronic charge $q$	$1.6 \times 10^{-19} \text{ C}$

field  $E$  to be normalized in such a way that its modulus square  $I = |E|^2$  is equal to the number of photons inside the cavity. The equation for the electric field can be written in terms of its optical intensity  $I$  and the phase  $\phi$  by defining  $E = \sqrt{I}e^{i\phi}$ . For simplicity, we retain the mean power of the spontaneous emission but neglect the explicit fluctuations terms. As the evolution equations for  $I$  and  $N$  do not depend on the phase  $\phi$ , we can concentrate only on the evolution of the former variables. The equations read

$$\frac{dI}{dt} = [G(N, I) - \gamma]I + 4\beta N \quad (1)$$

$$\frac{dN}{dt} = \frac{J}{q} - \gamma_N N - G(N, I)I \quad (2)$$

where  $G(N, I) = g_N(N - N_o)/(1 + \epsilon I)$  is the material gain. While the first term of the right-hand-side of (1) accounts for the stimulated emission and losses, the last one ( $4\beta N$ ) accounts for the mean value of the spontaneous emission in the lasing mode. This form for the spontaneous emission term has been largely used in the literature [4], [24]. Equations (1) and (2) are written in the reference frame in which the frequency is zero at threshold when spontaneous emission noise is neglected. The definition of the parameters and typical values appears in Table I. The threshold value for  $J$  ( $J_{th}$ ) is given by  $J_{th} = q\gamma_N N_{th}$ , where  $N_{th} = N_o + \gamma/g_N$ . The dynamics of these equations for constant  $J > J_{th}$  is such that both  $I$  and  $N$  relax to their steady states by performing damped oscillations [4], [23]. The frequency  $\omega_0$  of these oscillations close to the steady state can be calculated linearizing the equations of motion. For the simplest case ( $\epsilon = \beta = 0$ ), one obtains  $\omega_0 = \sqrt{g_N(J - J_{th})/q} \approx 25 \text{ ns}^{-1}$  ( $f_0 \equiv \omega_0/2\pi \approx 4 \text{ GHz}$ ) for the previous parameter values and  $J = 1.23J_{th}$ .

The purpose of this work is to study the dynamics of (1) and (2) under modulation. In particular, we will consider modulations mainly in the pump current  $J$ , but also in the losses  $\gamma$ , which would be an option in DBR or multisection lasers. A detailed description of the qualitative features of the behavior when the pump is modulated in the form

$$J \rightarrow J_b[1 + \delta \cos(\omega_m t)] \quad (3)$$

where  $J_b$  is a fixed value of the current (bias current), such that  $J_b > J_{th}$ , can be found in [25]. When  $J$  becomes time dependent, a very rich dynamical structure can appear depending on the values of the amplitude,  $\delta$  ( $\delta < 1$  to satisfy the physical

constraint that the total current has to be positive), and the frequency,  $\omega_m$ , of the modulation. For small values of  $\delta$  and for  $\omega_m$  smaller than the  $-3$  dB modulation bandwidth, the system behaves almost as a linear oscillator with damping terms: it periodically oscillates with the frequency  $\omega_m$  of the input current. Moreover, the response  $I_{\max}$  (maximum value of the optical intensity) has a maximum at the relaxation oscillation frequency  $\omega_0$  (linear resonance [26]).

In large amplitude modulation, strong nonlinear effects appear. In addition to a response at the same frequency of modulation  $\omega_m$  (with a maximum shifted to a smaller frequency), other frequencies can be excited for sufficiently high modulation amplitudes  $\delta$ . This gives rise to a more complex behavior for the response of the system, leading even to multistability (several stable responses for the same value of the input parameters). The possible responses can be classified as  $n/l$ , where  $n$  and  $l$  are integer numbers with no common factors, such that the response frequency is  $l\omega_m/n$ . The  $n/1$  responses are also called  $nT$ -periodic responses because the period of the resulting signal is  $n$  times larger than  $T_m$ , where  $T_m = 2\pi/\omega_m$  is the period of the external modulation. The existence of these responses can be visualized by plotting the amplitude  $I_{\max}$  of the stable  $n/l$  responses (whenever they exist) versus the modulation frequency  $\omega_m$  for fixed value of the modulation amplitude  $\delta$ . The resulting curves strongly depend on  $\delta$ .

- For very small  $\delta$ , the  $1T$  response is the only response present for all values of  $\omega_m$ .
- Increasing  $\delta$  [solid line of Fig. 1(a)], a decrease of the modulation frequency  $\omega_m$  generates a bistable region in which two different  $1T$  responses are possible.
- After a further increase of  $\delta$ , the  $2T$  response appears continuously, when decreasing  $\omega_m$  (starting from big values of  $\omega_m$ ), as a period doubling bifurcation of the  $1T$  response (see [25, Fig. 2] for temporal trajectories). The  $2T$  response around  $\omega_m/\omega_0 \approx 2.0$  is also known as a parametric resonance [26].
- For larger values of  $\delta$  [Fig. 1(b)], other  $nT$  responses with  $n > 2$  appear. Each of these  $nT$  responses exist for a given range of values of  $\omega_m$  and are unconnected to the previous  $1T$  and  $2T$  responses. At both ends of its frequency range, they disappear through saddle-node bifurcations.

Besides this general framework, all the existing  $nT$  responses can, at a given value of the modulation amplitude, suffer different types of period doubling bifurcations which, following the Feigenbaum route, can eventually lead to chaotic behavior [see dashed line in Fig. 1(b)].

For fixed modulation amplitude, each  $n/l$  response has its maximum at a given value of the modulation frequency. This maximum is called the  $n/l$  resonance. In this work, we are mainly interested in the  $n/1$  resonances (or  $nT$  resonances) because they usually yield the maximum output power. In the literature, they are also known as *main resonances* or *primary saddle-node resonances* because they coincide very accurately with some of the saddle-node bifurcations described before. These resonances are indicated by the solid dot symbols in Fig. 1.

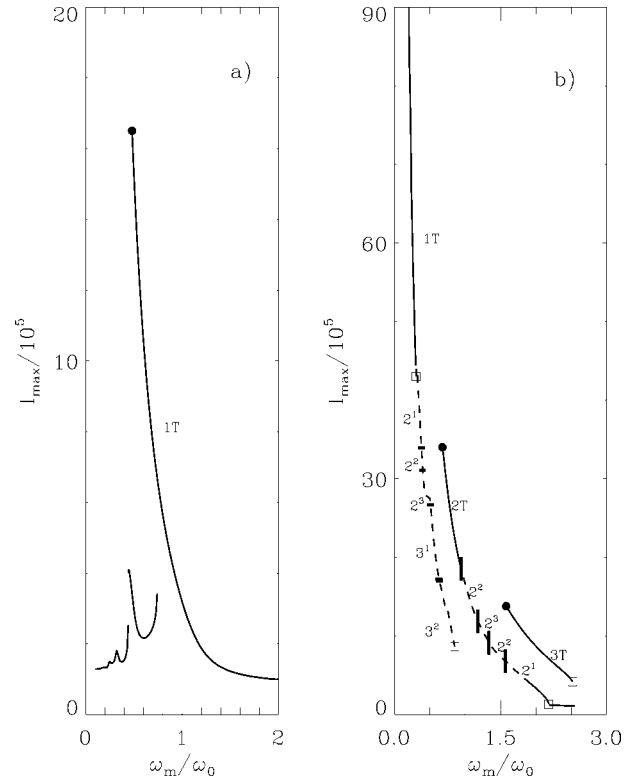


Fig. 1. Responses ( $I_{\max}$ ) versus the normalized external frequency  $\omega_m$  for different values of the modulation pump amplitude in the case  $J_b = 1.23J_{th}$ ,  $\epsilon = 0$ ,  $\beta = 0$ . Other parameters are as indicated in the text. (a)  $\delta = 0.1$ . (b)  $\delta = 0.3$ . The  $2^k$  and  $3^k$  responses correspond to further period doubling bifurcations.

The curves in the  $(\omega_m, \delta)$  plane joining the points at which  $nT$  resonances occur are called the *skeleton curves* for the  $nT$  resonances (in our case, the nonlinear oscillator given by the rate equations belongs to the class of *soft spring oscillators*). Our main effort will be directed to finding the skeleton lines for each main resonance of the  $nT$  type. This description can be of interest for the experimentalists to determine the resonance frequency at which the maximum response is obtained for a given external amplitude of the injection current.

### III. QUASI-CONSERVATIVE THEORY

Equations (1) and (2) can be reduced to a set of dimensionless equations by performing the following change of variables  $y = 2g_N I/\gamma$ ,  $z = g_N(N - N_o)/\gamma$ ,  $\tau = \gamma t/2$ , such that the equations become

$$\frac{dy}{d\tau} = 2 \left( \frac{z}{1 + \bar{s}y} - 1 \right) y + cz + d \quad (4)$$

$$\frac{dz}{d\tau} = a - bz - \frac{zy}{1 + \bar{s}y} \quad (5)$$

with new parameters defined as

$$a = \frac{2g_N}{\gamma^2} \left( \frac{J}{q} - \gamma_N N_o \right), \quad b = \frac{2\gamma_N}{\gamma}, \quad c = \frac{16\beta}{\gamma},$$

$$d = \frac{16\beta g_N N_o}{\gamma^2}, \quad \bar{s} = \frac{\epsilon\gamma}{2g_N}. \quad (6)$$

These evolution equations can be cast in the form

$$\frac{dy}{d\tau} = D_{12} \frac{\partial V}{\partial z} \quad (7)$$

$$\frac{dz}{d\tau} = -D_{12} \frac{\partial V}{\partial y} - D_{22} \frac{\partial V}{\partial z} \quad (8)$$

with the following *potential* function [23]:

$$V(y, z) = a_1 y + a_2 y^2 + a_3 \ln(y) + \frac{a_4}{y} + \frac{1}{2} \left[ z - 1 - \bar{s}y + \frac{(d + cz)}{2y} (1 + \bar{s}y) \right]^2 \quad (9)$$

where we have defined the functions

$$D_{12}(y, z) = \frac{4y^2}{(1 + \bar{s}y)[2y + c(1 + \bar{s}y)]} \quad (10)$$

$$D_{22}(y, z) = \frac{4y[(1 + 2\bar{s} + b\bar{s})y^2 + by + d + cz]}{(1 + \bar{s}y)[2y + c(1 + \bar{s}y)]^2} \quad (11)$$

and the coefficients

$$\begin{aligned} a_1 &= 1/2 - a\bar{s}/2 + b\bar{s} - \bar{s}d(1 + b\bar{s})/4 - a\bar{s}^2 c/4 \\ a_2 &= \bar{s}(1 + b\bar{s})/4 \\ a_3 &= -[a - b + (ac + bd)\bar{s} + d/2]/2 \\ a_4 &= (ac + bd)/4. \end{aligned} \quad (12)$$

The form of the equations (and the fact that  $D_{22} > 0$ ) proves that  $V(y, z)$  is a Lyapunov potential, i.e., it is a function that decreases monotonically along trajectories  $dV/dt \leq 0$ . This potential reduces to the one found for a Toda oscillator when the gain saturation parameter  $\epsilon$  and the spontaneous emission rate  $\beta$  are both equal to zero [27]. In the case where these two terms are different from zero, the potential is both quantitatively and qualitatively different from the Toda potential, mainly due to the effect of the spontaneous emission term  $\beta$ .

The decrease of the Lyapunov potential is due to the function  $D_{22}(y, z)$  appearing in the evolution equation (8). Therefore, in the dynamical equations, we can identify the conservative terms (those proportional to  $D_{12}$ ) and the dissipative ones (those proportional to  $D_{22}$ ). If the dissipative terms were not present, i.e., if  $D_{22} = 0$ , the potential would take a constant value  $E = V(y, z)$  and we would have a conservative system with periodic orbits. The frequency,  $\omega = 2\pi/T$ , of such an orbit of the conservative system is a function of the potential, i.e.,  $\omega = \omega(E)$ , that can be obtained, using standard methods of mechanics, as [23]

$$T = \int_{y_a}^{y_b} \frac{(1 + \bar{s}y) dy}{y[2(E - a_1 y - a_2 y^2 - a_3 \ln(y) - a_4 y^{-1})]^{1/2}} \quad (13)$$

where  $y_a < y_b$  are the values of  $y$  that cancel the denominator of the integrand. Notice that the periodic orbits, that we write as  $[y_0(\tau - \tau_0, E), z_0(\tau - \tau_0, E)]$ , depend on an initial time  $\tau_0$  and on the value of the Lyapunov potential  $E$ .

### A. Pump Modulation

We now include the modulation terms. We first consider the case of modulation in the pump as given in (3). In terms of the rescaled variables, (8) becomes

$$\frac{dz}{d\tau} = -D_{12} \frac{\partial V}{\partial y} - D_{22} \frac{\partial V}{\partial z} + A_m \cos(\bar{\omega}_m \tau) \quad (14)$$

with

$$A_m = \frac{2J_b \delta g_N}{q\gamma^2}, \quad \bar{\omega}_m = \frac{2}{\gamma} \omega_m. \quad (15)$$

We look for  $nT$  responses, i.e., periodic solutions  $[y^{(n)}(\tau), z^{(n)}(\tau)]$  of (7) and (14) with a frequency  $\omega_n = \bar{\omega}_m/n$  or, equivalently, with a period  $T_n = nT_m = n2\pi/\bar{\omega}_m$ . In this case, the potential function  $V(y, z)$  is no longer a constant of motion. However, for a periodic orbit, it is still true that the integral of  $dV = [(\partial V/\partial y)\dot{y} + (\partial V/\partial z)\dot{z}] d\tau$  over a period is equal to zero. By using this property and after replacing in the previous expression  $\dot{y}$  and  $\dot{z}$  coming from (7) and (14), we obtain that the periodic solutions must satisfy the condition

$$\begin{aligned} A_m \int_0^{T_n} d\tau V_z(y^{(n)}(\tau), z^{(n)}(\tau)) \cos(\bar{\omega}_m \tau) \\ = \int_0^{T_n} d\tau D_{22}(y^{(n)}(\tau), z^{(n)}(\tau)) \\ \cdot [V_z(y^{(n)}(\tau), z^{(n)}(\tau))]^2 \end{aligned} \quad (16)$$

where  $V_z$  stands for  $\partial V/\partial z$ . The quasi-conservative theory assumes that the periodic orbits  $[y^{(n)}(\tau), z^{(n)}(\tau)]$  can be approximated, near the resonance, by conservative orbits  $[y_0(\tau - \tau_0, E_n), z_0(\tau - \tau_0, E_n)] \equiv [y_n(\tau - \tau_0), z_n(\tau - \tau_0)]$ , corresponding to the value of the potential  $E_n$  that yields the desired frequency  $\omega_n = \omega(E_n)$ . Substitution of this ansatz in the above equation leads to

$$\begin{aligned} A_m \int_0^{T_n} d\tau V_z(y_n(\tau), z_n(\tau)) \cos(\bar{\omega}_m(\tau + \tau_0)) \\ = \int_0^{T_n} d\tau D_{22}(y_n(\tau), z_n(\tau)) [V_z(y_n(\tau), z_n(\tau))]^2. \end{aligned} \quad (17)$$

By defining  $R_n, S_n, \theta_n$  by

$$\begin{aligned} R_n &= \int_0^{T_n} d\tau D_{22}(y_n(\tau), z_n(\tau)) \\ &\quad \cdot [V_z(y_n(\tau), z_n(\tau))]^2 \\ S_n \begin{Bmatrix} \sin(\theta_n) \\ \cos(\theta_n) \end{Bmatrix} &= \int_0^{T_n} d\tau V_z(y_n(\tau), z_n(\tau)) \begin{Bmatrix} \sin(\bar{\omega}_m \tau) \\ \cos(\bar{\omega}_m \tau) \end{Bmatrix} \end{aligned} \quad (18)$$

we arrive at

$$A_m \cos(\bar{\omega}_m \tau_0 + \theta_n) = \frac{R_n}{S_n}. \quad (19)$$

According to this equation, for given  $A_m$  and  $\bar{\omega}_m$ , there exist at most  $2n$  different orbits of period  $nT_m$ . They correspond to the functions  $[y_0(\tau - \tau_0, E_n), z_0(\tau - \tau_0, E_n)]$  for the  $2n$  values of  $\tau_0 = (\alpha_n + k\pi)/\bar{\omega}_m, k = 0, \dots, 2n - 1$  and

$\alpha_n = \arccos(R_n/(S_n A_m)) - \theta_n$ . It turns out that  $n$  of these solutions are unstable, while the remaining stable ones correspond, in fact, to trivial translations by a time amount  $\bar{T}_m$  of the same basic solution (pulse position multistability [2], [20]). Therefore, for a given value of  $A_m$  and  $\bar{\omega}_m$ , there is just one corresponding stable orbit of the conservative system. Alternatively, we can look at the previous equation as a condition for the existence of periodic orbits. For a given modulation frequency  $\bar{\omega}_m$ , there will exist periodic orbits of period  $n\bar{T}_m$  if the amplitude of the modulation verifies  $A_m \geq R_n/S_n$ . Since resonances almost coincide in this case with the limit of existence of periodic orbits (see Fig. 1 and the discussion of the previous section), this criterion implies that the skeleton curves for the  $nT$  resonance are

$$A_m = \frac{R_n}{S_n}. \quad (20)$$

In practice, it is difficult to find solutions of the conservative motion  $[y_0(\tau, E), z_0(\tau, E)]$  analytically and one performs a numerical integration of the conservative system in order to find the quantities  $R_n, S_n$ . However, in the simple case of  $\epsilon = 0$  and  $\beta = 0$ , (17) can be simplified by replacing  $V_z$  with help of (7) and yielding

$$A_m \int_0^{T_n} d\tau \dot{x}_n(\tau) \cos(\bar{\omega}_m(\tau + \tau_0)) \\ = \int_0^{T_n} d\tau [b + y_{st} \exp(x_n(\tau))] \dot{x}_n(\tau)^2 / 2 \quad (21)$$

where  $x_0 \equiv \ln(y_0/y_{st})$ ,  $y_{st} = a - b$  is the steady-state value of  $y$  in the absence of modulation, and  $x_0$  is a periodic function of frequency  $w_n$  that can be written as a Fourier series in the form:  $x_n(\tau) = x_0(\tau, E_n) = Q_0/2 + \sum_{k=1}^{\infty} Q_k \cos[kw_n(\tau + \mu_k)]$ . Using this expression, and after simple algebra, the integrals of (22) can be performed, giving rise to

$$A_m \sin[n\omega_n(\mu_n - \tau_0)] = \frac{a}{2} \omega_n \frac{\sum_{k=1}^{\infty} Q_k^2 k^2}{nQ_n}. \quad (22)$$

As discussed earlier, the  $nT$  resonances are obtained for  $\sin[n\omega_n(\mu_n - \tau_0)] = 1$ , i.e.,

$$A_m = \frac{a}{2} \omega_n \frac{\sum_{k=1}^{\infty} Q_k^2 k^2}{nQ_n}. \quad (23)$$

This expression has the advantage that the contribution of each coefficient in the Fourier series of  $x_0$  appears explicitly. In particular, it is seen that  $nT$  resonance may be excited by a finite amplitude of the external modulation only if the  $n$ th harmonic of the conservative solution is nontrivial. Therefore, this effect can be considered as harmonic locking of the fundamental relaxation oscillation by an external modulation.

In the case  $\epsilon \neq 0$  and  $\beta \neq 0$  it is still possible to use a series expansion for the variable  $x_0$ , and to obtain an expression in terms of the Fourier coefficients. However, the resulting expression is so complicated, in the sense that in the denominator different coefficients of the Fourier expansion contribute, that we

find simpler instead to use (20) to obtain the theoretical skeleton curve.

### B. Loss Modulation

Let us turn now to loss modulation. We consider (1) and (2) with a fixed value of the current  $J$  but modulated loss term<sup>4</sup>

$$\gamma \rightarrow \gamma[1 + \gamma_m \cos(w_m t)]. \quad (24)$$

The reduced equations for  $y$ , (7), can be written as

$$\frac{dy}{d\tau} = D_{12} \frac{\partial V}{\partial z} - 2y\gamma_m \cos(\bar{\omega}_m \tau) \quad (25)$$

while (8) remains unchanged. It is straightforward now to extend the QCT to this case. Proceeding as in the case of pump modulation, we arrive at

$$\gamma_m \cos(\bar{\omega}_m t_0 + \theta'_n) = \frac{R_n}{S'_n} \quad (26)$$

where  $R_n$  is given by (18) and  $S'_n$  is

$$S'_n \begin{Bmatrix} \sin(\theta'_n) \\ \cos(\theta'_n) \end{Bmatrix} = -2 \int_0^{T_n} d\tau y_n(\tau) V_y(y_n, z_n) \begin{Bmatrix} \sin(\bar{\omega}_m \tau) \\ \cos(\bar{\omega}_m \tau) \end{Bmatrix}.$$

$V_y(y_n, z_n)$  stands for  $\partial V / \partial y(y_n(\tau), z_n(\tau))$ . The skeleton curves are then given by

$$\gamma_m = \frac{R_n}{S'_n}. \quad (27)$$

In the case  $\epsilon = 0$  and  $\beta = 0$ , an expression in terms of Fourier series, similar to (23), can be derived as follows:

$$\gamma_m = \frac{a}{2} \frac{\sum_{k=1}^{\infty} Q_k^2 k^2}{n^2 Q_n}. \quad (28)$$

This expression is equivalent to the one obtained in [16], where a laser with periodic modulation of losses, but neglecting the spontaneous emission and gain saturation terms, is studied in detail. Again for  $\epsilon$  and  $\beta$  different from zero, we need to solve (27) numerically.

## IV. RESULTS

Intensive numerical simulations have been performed in [25] in order to obtain the maximum responses of the system for different  $\delta$  and  $w_m$  in order to compare with the analytical expressions derived in the previous section. In principle, for a given  $\delta$ , one should find the value of  $w_m$  that maximizes the response at each  $nT$  resonance. However, this is a very lengthy procedure that can be avoided by finding, instead, the value of  $w_m$  where a saddle-node bifurcation is born, since we have observed that the maximum response appears just before the solution becomes unstable. This allows us to identify the position of the maximum response in the  $(w_m, \delta)$  plane with the position of the bifurcation. The procedure of finding such bifurcations is easier to implement using nonlinear dynamical tools than to perform the

<sup>4</sup>Cavity loss in lasers can be modulated in practice by different ways, for example by using a variable reflector or in a two-section laser when modulating periodically the passive section.

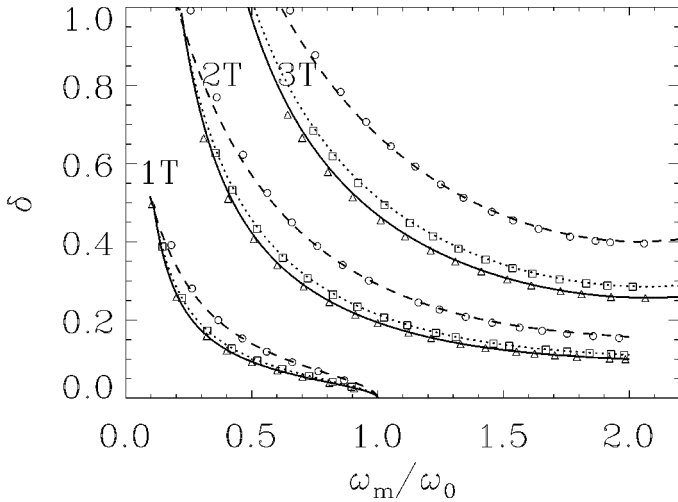


Fig. 2. Maxima of main resonances in the plane  $(\omega_m/\omega_0, \delta)$  for pump modulation. Effect of  $\epsilon$ . Analytical results (20):  $\epsilon = 0$  (solid line),  $\epsilon = 6 \times 10^{-9}$  (dotted line),  $\epsilon = 3 \times 10^{-8}$  (dashed line). Numerical results:  $\epsilon = 0$  (triangles),  $\epsilon = 6 \times 10^{-9}$  (squares),  $\epsilon = 3 \times 10^{-8}$  (circles).  $\beta = 0$ . Other parameters as in Fig. 1.

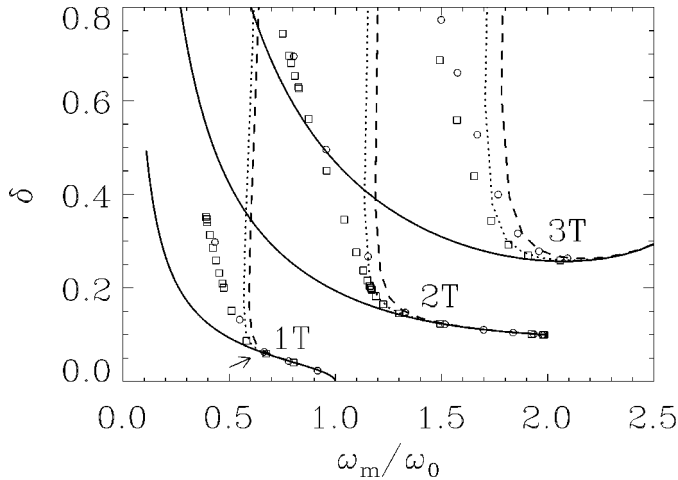


Fig. 3. Maxima of main resonances in the plane  $(\omega_m/\omega_0, \delta)$  for pump modulation. Effect of  $\beta$ . Analytical results (20):  $\beta = 0$  (solid line),  $\beta = 6.2 \times 10^{-11} ps^{-1}$  (dotted line),  $\beta = 2.2 \times 10^{-10} ps^{-1}$  (dashed line). Numerical results (19):  $\beta = 6.2 \times 10^{-11} ps^{-1}$  (squares),  $\beta = 2.2 \times 10^{-10} ps^{-1}$  (circles).  $\epsilon = 0$ . Other parameters as in Fig. 1. Marked with an arrow the cut-off value  $\omega_c$ .

whole simulations of the rate equations [28]. The comparison has been performed using the typical values for the parameters explained in Section II. Similar results hold for other parameter values.

We compare in Figs. 2 and 3 the predictions of the QCT in the case of pump modulation, as given by (20), with the numerical simulations. In order to perform this comparison, the skeleton curves have been plotted in terms of the original variables  $\delta$  and  $\omega_m$  by using (6) and (15). Fig. 2 gives evidence that the theoretical predictions coincide with the numerical results with a great degree of accuracy in the case  $\epsilon = 0$  and  $\beta = 0$ . This figure also shows that a similar agreement between the theory and simulations can be observed for the case of  $\epsilon \neq 0$ , but  $\beta = 0$  still. In this case, the role of the gain saturation parameter  $\epsilon$  is such that, for a fixed value of the frequency  $\omega_m$ , a larger value of modulation amplitude  $\delta$  is needed to obtain the optimal periodic

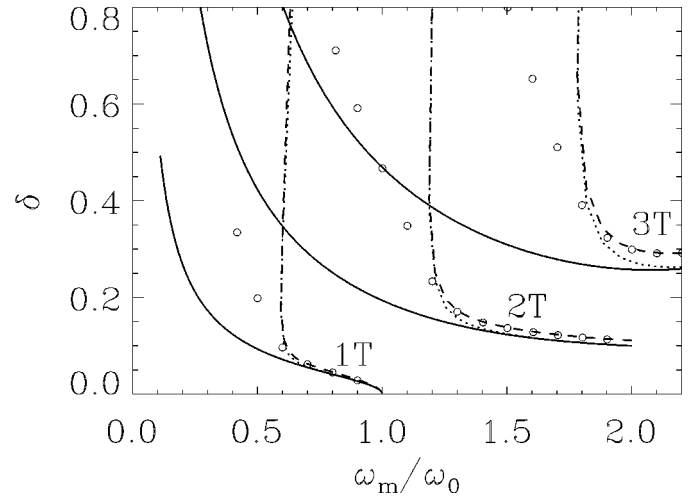


Fig. 4. Maxima of main resonances in the plane  $(\omega_m/\omega_0, \delta)$  for pump modulation. Combined effect of  $\beta$  and  $\epsilon$ . Analytical results (20):  $\beta = 0, \epsilon = 0$  (solid line),  $\beta = 6.2 \times 10^{-11} ps^{-1}, \epsilon = 0$  (dotted line),  $\beta = 6.2 \times 10^{-11} ps^{-1}, \epsilon = 6 \times 10^{-9}$  (dashed line). Numerical results (19):  $\beta = 6.2 \times 10^{-11} ps^{-1}, \epsilon = 6 \times 10^{-9}$  (circles). Other parameters are as in Fig. 1.

response for each main resonance. The effect is quantitatively more important for higher order resonances,  $n > 1$ . Qualitatively, we can understand this effect as a result of the increase in dissipation produced by the increase of the saturation term.

More dramatic is the effect of the spontaneous emission term  $\beta$ . In Fig. 3, we can see that small values of the noise rate  $\beta$  strongly modify the skeleton curves for modulation frequencies  $\omega_m$  smaller than a cut-off value  $\omega_c$  (marked with an arrow in the figure), whereas they remain basically unchanged for  $\omega_m > \omega_c$ . For small  $\omega_m$ , the effect of  $\beta$  is such that much larger values of the modulation amplitude  $\delta$  are needed in order to find the optimal response for a given value of the modulation frequency  $\omega_m$ . In the absence of spontaneous emission  $\beta = 0$ , the tendency to decrease the main resonance frequency with increasing amplitude of modulation can be understood by noticing that the number of photons is not limited from below. On the contrary, when  $\beta \neq 0$ , a spontaneous emission background is created and, during the modulation period, the number of photons cannot be smaller than this value and, consequently, the response is maintained basically unchanged at any smaller frequency. In this case, a nonresonant regime of gain switching dominates.

The theoretical prediction behaves qualitatively in the same way and predicts correctly the cut-off frequency. However, it predicts a much sharper increase of the optimal modulation amplitude. This could be explained as follows: while the period of the conservative solutions always increases when the energy increases in the absence of spontaneous emission terms, as it can be seen from (13), the presence of the spontaneous emission noise terms introduces a maximum in the resulting expression of the period as function of the energy. This fact forbids the conservative orbits with a frequency smaller than the cut-off frequency. This means that the conservative orbit we are using can be very different from the orbit followed by the modulated system. For smaller values of  $\beta$ , the boundary approaches to the one for the case  $\beta = 0$ , as expected. Finally, in Fig. 4, the combined effect of  $\epsilon$  and  $\beta$  is shown. The same qualitative effect that was already explained also appears for other values of the bias

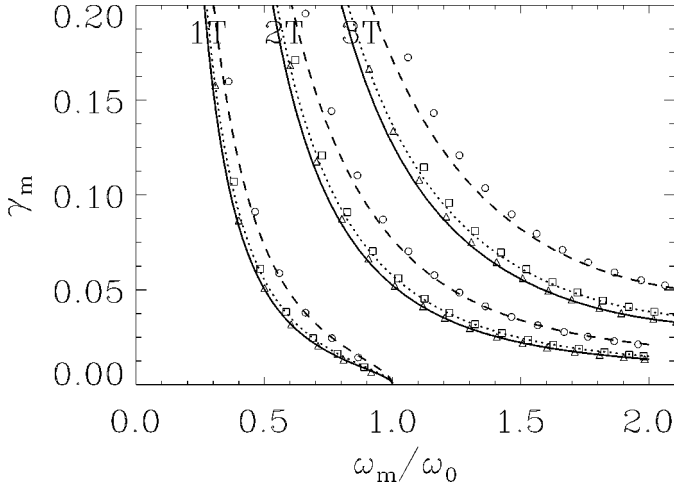


Fig. 5. Maxima of main resonances in the plane  $(\omega_m/\omega_0, \delta)$  for loss modulation. Effect of  $\epsilon$ . Analytical results (27):  $\epsilon = 0$  (solid line),  $\epsilon = 6 \times 10^{-9}$  (dotted line),  $\epsilon = 3 \times 10^{-8}$  (dashed line). Numerical results (20):  $\epsilon = 0$  (triangles),  $\epsilon = 6 \times 10^{-9}$  (squares),  $\epsilon = 3 \times 10^{-8}$  (circles).  $\beta = 0$ . Other parameters are as in Fig. 1.

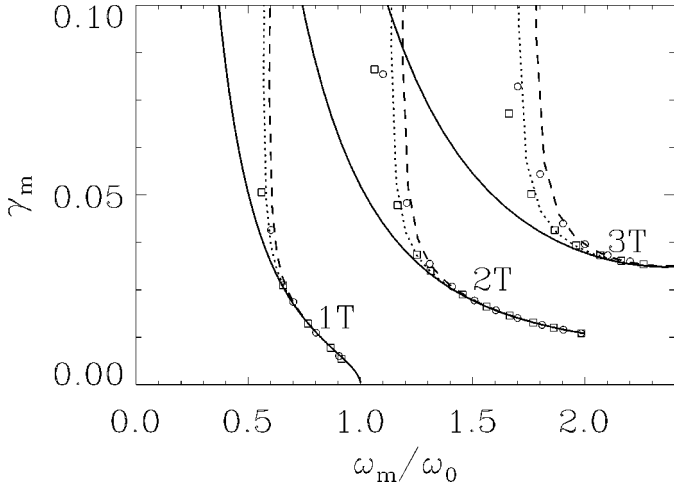


Fig. 6. Maxima of main resonances in the plane  $(\omega_m/\omega_0, \delta)$  for loss modulation. Effect of  $\beta$ . Analytical results (27):  $\beta = 0$  (solid line),  $\beta = 6.2 \times 10^{-11} ps^{-1}$  (dotted line),  $\beta = 2.2 \times 10^{-10} ps^{-1}$  (dashed line). Numerical results (19):  $\beta = 6.2 \times 10^{-11} ps^{-1}$  (squares),  $\beta = 2.2 \times 10^{-10} ps^{-1}$  (circles).  $\epsilon = 0$ . Other parameters are as in Fig. 1.

current  $J_b$ . For  $J_b > 1.23J_{th}$ , the same boundaries appear but for larger values of  $m$ . This effect was experimentally reported in [3], where it is indicated that higher order bifurcations are more likely to occur for smaller DC bias levels than for higher ones.

For the case of loss modulation, the analytical and numerical results coincide for  $\epsilon = 0$  and  $\beta = 0$ , and for the case  $\epsilon \neq 0$  and  $\beta = 0$ , analogously to that of the pump modulation case (see Fig. 5). However, when the spontaneous emission term is introduced, the boundaries obtained numerically also depart from the analytical predictions (see Figs. 6 and 7).

We have observed that it is possible to obtain an interesting relationship between the effect produced by loss modulation and pump modulation. The relation can be obtained more clearly if we write the evolution equation for the variable  $x = \ln(y/y_{st})$ , defined in terms of the stationary value  $y_{st}$  of the variable  $y$  in

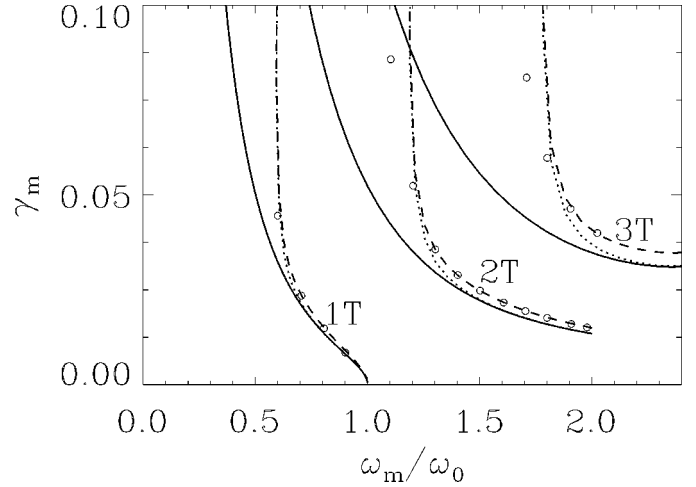


Fig. 7. Maxima of main resonances in the plane  $(\omega_m/\omega_0, \delta)$  for loss modulation. Combined effect of  $\beta$  and  $\epsilon$ . Analytical results (27):  $\beta = 0, \epsilon = 0$  (solid line),  $\beta = 6.2 \times 10^{-11} ps^{-1}, \epsilon = 0$  (dotted line),  $\beta = 6.2 \times 10^{-11} ps^{-1}, \epsilon = 6 \times 10^{-9}$  (dashed line). Numerical results (19):  $\beta = 6.2 \times 10^{-11} ps^{-1}, \epsilon = 6 \times 10^{-9}$  (circles). Other parameters are as in Fig. 1.

the absence of modulation. For small  $\beta, \epsilon$ , it is  $y_{st} \approx a - b$ . It turns out that the resulting equations in the case of modulation in the pump or in the losses take basically the same form, namely

$$\ddot{x} + \dot{x}^2 G_1(x) + \dot{x} G_2(x) + G_3(x) = F_{P,L}(x, \tau) \quad (29)$$

where  $G_1(x), G_2(x)$ , and  $G_3(x)$  are given functions of  $x$  whose detailed expressions are not needed here. The only difference is in the right-hand side of this equation which, for the case of modulation in the pump, is

$$F_P(x, \tau) = A_m \cos(\bar{\omega}_m \tau) F_1(x) \quad (30)$$

$$F_1(x) = \frac{2}{1 + \bar{y}_{st} \exp(x)} + \frac{c}{y_{st} e^x}$$

while in the case of modulation in the losses, it is

$$F_L(x, \dot{x}, \tau) = 2\gamma_m \bar{\omega}_m \sin(\bar{\omega}_m \tau) - 2\gamma_m \cos(\bar{\omega}_m \tau) F_2(x, \dot{x})$$

$$F_2(x, \dot{x}) = b + \frac{y_{st} \exp(x)}{1 + \bar{y}_{st} \exp(x)} + \dot{x} \left[ \frac{2\bar{y}_{st}^2 e^{2x} + c(1 + \bar{y}_{st} e^x)^2}{(1 + \bar{y}_{st} e^x)[2y_{st} e^x + c e^{2x}(1 + \bar{y}_{st} e^x)]} \right]. \quad (31)$$

It is easy to see that the term containing  $F_2$  is negligible compared to the first contribution to  $F_L(x, \dot{x}, \tau)$ . In fact, if we consider the value of  $F_2$  in the steady state in the absence of modulation  $x = \dot{x} = 0$ , we obtain  $F_2 \approx a$ . A typical value is  $a \approx 0.01$ , while the product  $\gamma_m \bar{\omega}_m$  is of order 1 for  $\omega_m \sim \omega_0$ . If we now replace  $F_1(x)$  by its steady-state value  $F_1(0)$ , approximate the term  $1 + \bar{y}_{st} \approx 1$ , and neglect the term proportional to  $c$ , we arrive at

$$F_P \approx 2A_m \cos(\bar{\omega}_m \tau) \quad (32)$$

$$F_L \approx 2\gamma_m \bar{\omega}_m \sin(\bar{\omega}_m \tau). \quad (33)$$

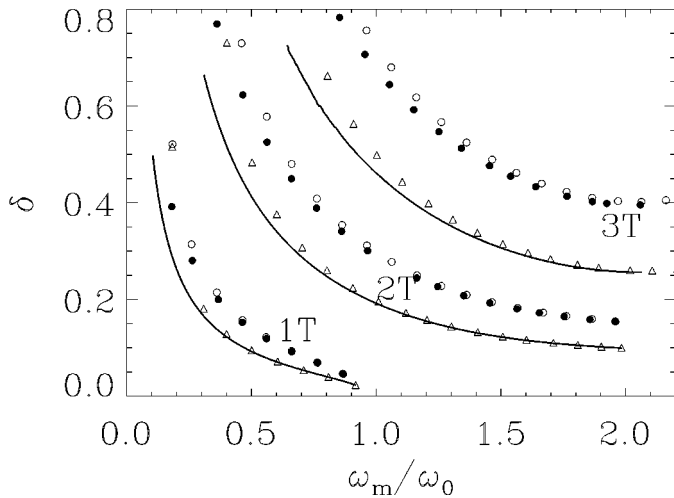


Fig. 8. Maxima of main resonances in the plane  $(\omega_m/\omega_0, \delta)$ . Numerical results. Pump modulation:  $\epsilon = 0$  (solid line) (equivalent to theoretical results),  $\epsilon = 3 \times 10^{-8}$  (filled circles). Loss modulation multiplied by factor of (34):  $\epsilon = 0$  (triangles),  $\epsilon = 3 \times 10^{-8}$  (circles).  $\beta = 0$ ,  $J_b = 1.23J_{th}$ .

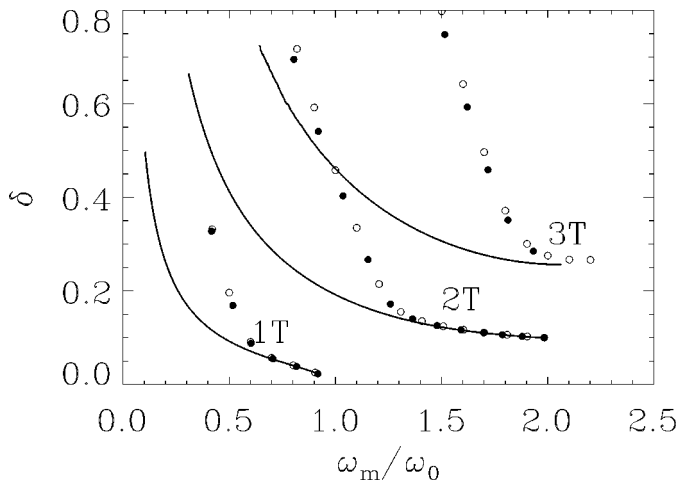


Fig. 9. Maxima of main resonances in the plane  $(\omega_m/\omega_0, \delta)$ . Numerical results. Pump modulation:  $\beta = 0$  (solid line),  $\beta = 2.2 \times 10^{-10} ps^{-1}$  (filled circles). Loss modulation multiplied by factor of (34):  $\beta = 2.2 \times 10^{-10} ps^{-1}$  (circles).  $\epsilon = 0$ ,  $J_b = 1.23J_{th}$ .

Therefore, we conclude that the role of the modulation in the pump is equivalent to the modulation in the losses, besides a trivial phase shift, if  $A_m = \gamma_m \bar{\omega}_m$ . In terms of the physical parameters, this is equivalent to

$$\delta = \gamma_m \omega_m \frac{\gamma q}{g_N J_b}. \quad (34)$$

This result shows that modulation in the pump or in the losses produces equivalent results if the respective modulation amplitudes are conveniently rescaled. It is possible to arrive at this result directly, in the case  $\epsilon = \beta = 0$ , by comparing the expressions in terms of Fourier coefficients (23) and (28). The validity of this equivalence of modulation in the pump and in the losses is shown in Figs. 8 and 9, where we compare, for typical values of  $\epsilon$  and  $\beta$ , the skeleton lines in the case of pump and loss modulation after the latter have been rescaled according to (34). It is clear from these figures that the proposed equivalence after parameter rescaling works well in the cases that have been shown.

A similar agreement is observed for other boundaries and values of the parameters.

Since relation (34) implies, for typical values of the parameters that  $\delta > \gamma_m$ , we recover the known results that loss modulation is more efficient to get bifurcations and chaos. This relation can be applied in the large-modulation signal regime (nonlinear regime), and hence it can be considered as an extension of previous analytical results in the case of the linear regime [29].

## V. COMPARISON TO EXPERIMENTS

The fingerprint of  $nT$  resonance regimes, which distinguish them from nonresonance  $nT$  periodic windows in chaos, is a dominant  $\omega_m/n$  component in microwave spectra. In particular, the  $\omega_m/2$  component in microwave spectra was dominating in the observations of [3] and [6], pointing out the resonance  $2T$  regime, that in the time domain leads to sharp spikes (no intermediate spikes at interval  $2T_m$ ). A direct example of the resonant  $2T$  regime observation and possible applications to all-optical clock division can be found in [30].

According to our predictions, resonant regimes with  $n > 2$  also exist in the system. However, they are dynamical isolates that cannot be observed with smooth sweeping of modulation parameters, besides the special cases of pulse excitation [18], [20], [21] or chaotic crisis on the basic  $1T$  periodic branch leading to switching to a  $3T$  branch as it was observed in [3] and explained in [31], [32].

Particularly relevant to our work is the paper by Liu and Ngai [3], where the response of a single-mode DFB laser subjected to current modulation is considered. We summarize the observations they obtain when changing the modulation frequency and amplitude of the RF signal and compare them to our results, as follows.

- 1) For small modulation frequency, there is only a  $1T$  period response for any signal amplitude. It was visualized in our system, in Fig. 2, for  $\omega_m/\omega_0 < 0.2$ , for  $\delta < 1$ .
- 2) For intermediate modulation frequency, there is a transition from  $1T$  to  $2T$  responses when increasing the modulation amplitude. This fact is seen in Fig. 2 in the region  $0.2 < \omega_m/\omega_0 < 2$ , for the corresponding values of  $\delta$ .
- 3)  $3T$  and  $4T$  solutions appear for large enough modulation frequency and amplitude. We find these solutions also in the case of sufficiently large values of the modulation frequency and amplitude (see Figs. 2–4). The  $4T$  solution would appear for larger values of the amplitude not plotted in the figure. We have checked that, for  $\epsilon = 0$  and  $\beta = 0$ , the corresponding  $4T$  boundary for pump modulation would have its minimum value at  $\omega_m/\omega_0 \sim 2.3$  and  $\delta \sim 0.4$ . However, identification of the  $3T$  branch observed in [3] is still hard to make as resonant due to the fact that the microwave spectra gives a dominate modulation component at  $\omega_m$ , but not at the subharmonic  $\omega_m/3$  as it might be expected for a purely resonant regime.

## VI. CONCLUSIONS

We have undertaken an analytical study to identify the optimal responses of a semiconductor laser subjected to an external periodic modulation in the pump of relative amplitude  $\delta$

and frequency  $\omega_m$ . We have computed the lines in the  $(\omega_m, \delta)$  plane that give a maximum response for each type of  $nT$  resonance (skeleton lines) and compared them to the numerical results reported in our previous paper [33]. The influence of saturation and spontaneous emission terms on the dynamics has also been examined. We have found that these specific laser diode parameters increase the thresholds of instabilities in the system, a fact that can be interpreted as an effect of the increase in the damping of relaxation oscillations. A qualitative comparison with experiments has also been performed. The analytical results we have obtained by an application of the quasiconservative theory allow us to explain satisfactorily the effect of the saturation term. The role of the gain saturation parameter is such that, for a fixed value of the frequency  $\omega_m$ , a larger value of modulation amplitude  $m$  is needed to obtain the optimal periodic response for each main resonance. This effect is more important for higher order resonances. However, the effect of the spontaneous emission term in the skeleton lines has not been completely explained by the analytical results and the discrepancy between the numerical and analytical results is due to the form of the conservative solution.

Loss modulation has also been considered and analytical and numerical results are in reasonable agreement. Furthermore, we have obtained a relation that shows the equivalence between pump and loss modulation. This equivalence relation, having a large validity for the numerical boundaries, allows the boundary limits for pump (or loss) modulation to be computed if the loss (pump) boundaries are known. We have recovered the known results that loss modulation is more efficient to get bifurcations and chaos than pump modulation.

## REFERENCES

- [1] H. Kawaguchi, *Bistabilities and Nonlinearities in Laser Diodes*. Norwood, MA: Artech House, 1994.
- [2] D. F. G. Gallagher, I. H. White, J. E. Carroll, and R. G. Plumb, "Gigabit pulse position bistability in semiconductor lasers," *L. Lightwave Technol.*, vol. LT-5, pp. 1391–1398, 1987.
- [3] H. F. Liu and W. F. Ngai, "Nonlinear dynamics of a directly modulated 1.55  $\mu\text{m}$  InGaAsP distributed feedback semiconductor laser," *IEEE J. Quantum Electron.*, vol. 29, pp. 1668–1675, 1993.
- [4] C. R. Mirasso, P. Colet, and M. San Miguel, "Dependence of timing jitter on bias level for single-mode semiconductor lasers under high speed operation," *IEEE J. Quantum Electron.*, vol. 29, pp. 23–32, 1993.
- [5] C. R. Mirasso, P. Colet, and P. García-Fenández, "Synchronization of chaotic semiconductor lasers: Application to encoded communications," *Photon. Technol. Lett.*, vol. 8, pp. 299–301, 1996.
- [6] Y. Matsui, S. Kutsuzawa, S. Arahira, Y. Ogawa, and A. Suzuki, "Bifurcation in 20-GHz gain-switched 1.55- $\mu\text{m}$  MQW lasers and its control by CW injection seeding," *IEEE J. Quantum Electron.*, vol. 34, pp. 1213–1223, 1998.
- [7] M. Tang and S. Wang, "Simulation studies of bifurcation and chaos in semiconductor lasers," *Appl. Phys. Lett.*, vol. 48, pp. 900–902, 1986.
- [8] E. Hemery, L. Chusseau, and J. M. Lourtioz, "Dynamical behaviors of semiconductor lasers under strong sinusoidal current modulation: Modeling and experiment at 1.3 $\mu\text{m}$ ," *IEEE J. Quantum Electron.*, vol. 26, pp. 633–641, 1990.
- [9] Y. H. Kao and H. T. Lin, "Virtual Hopf precursor of period-doubling route in directly modulated semiconductor lasers," *IEEE J. Quantum Electron.*, vol. 29, pp. 1617–1623, 1993.
- [10] G. P. Agrawal, "Effect of gain nonlinearities on period-doubling and chaos in directly modulated semiconductor lasers," *Appl. Phys. Lett.*, vol. 49, pp. 1013–1015, 1986.
- [11] M. Tang and S. Wang, "Simulation studies of dynamical behavior of semiconductor laser with Auger recombination," *Appl. Phys. Lett.*, vol. 50, pp. 1861–1863, 1987.
- [12] C. G. Lim, S. Iezekiel, and C. M. Snowden, "Is noise a crucial factor in rate equation modeling of nonlinear dynamics in laser diodes?," *Appl. Phys. Lett.*, vol. 77, pp. 3493–3495, 2000.
- [13] T. H. Yoon, C. H. Lee, and S. Y. Shing, "Perturbation analysis of bistability and period doubling in directly-modulated laser diodes," *IEEE J. Quantum Electron.*, vol. 25, pp. 1993–2000, 1989.
- [14] Y. Hori, H. Serizawa, and H. Sato, "Chaos in a directly modulated semiconductor laser," *J. Opt. Soc. Amer. B*, vol. 5, pp. 1128–1132, 1988.
- [15] T. Erneux, S. M. Baer, and P. Mandel, "Subharmonic bifurcation and bistability of periodic solutions in a periodically modulated laser," *Phys. Rev. A*, vol. 35, pp. 1165–1171, 1987.
- [16] A. M. Samson and S. I. Turovets, "Hierarchy of bifurcations in a laser with periodic modulation of losses," *Doklady AN BSSR*, vol. 31, pp. 888–890, 1987.
- [17] I. B. Schwartz, "Infinite primary saddle-node bifurcation in periodically forced systems," *Phys. Lett. A*, vol. 126, pp. 411–418, 1988.
- [18] A. M. Samson, Yu. A. Logvin, and S. I. Turovets, "The role of potential symmetry and shape of a nonlinear oscillator in the bifurcation hierarchy for harmonic action," *Sov. Radiophys. and Quantum Electron.*, vol. 33, pp. 40–50, 1990.
- [19] I. B. Schwartz and T. Erneux, "Subharmonic hysteresis and period doubling bifurcations for a periodically driven laser," *SIAM J. Appl. Math.*, vol. 54, pp. 1083–1100, 1994.
- [20] V. N. Chizhevsky and S. I. Turovets, "Periodically loss-modulated CO<sub>2</sub> laser as an optical amplitude and phase multitrigger," *Phys. Rev. A*, vol. 50, pp. 1840–1843, 1994.
- [21] V. N. Chizhevsky, "Coexisting attractors in a CO<sub>2</sub> laser with modulated losses," *J. Opt. B: Quantum Semiclass. Opt.*, vol. 2, pp. 711–717, 2000.
- [22] A. M. Katz, "Forced oscillations in the quasiconservative nonlinear systems with one degree of freedom" (in Russian), *Prikladnaya Matematika i Mekhanika*, vol. 19, pp. 13–32, 1955.
- [23] C. Mayol, R. Toral, and C. R. Mirasso, "Lyapunov potential description for laser dynamics," *Phys. Rev. A*, vol. 59, pp. 4690–4698, 1999.
- [24] P. Spano, A. Mecozzi, A. Sapia, and A. D'Ottavi, "Noise and transient dynamics in semiconductor lasers," in *Springer Proceedings in Physics*. Berlin: Springer-Verlag, 1991, vol. 55, Nonlinear Dynamics and Quantum Phenomena in Optical Systems.
- [25] C. Mayol, S. I. Turovets, R. Toral, C. R. Mirasso, and L. Pesquera, "Main resonances in directly modulated semiconductor lasers: Effect of spontaneous emission and gain saturation," *IEE Proc.—Optoelectron.*, vol. 148, pp. 41–45, 2001.
- [26] E. A. Jackson, *Perspectives of Nonlinear Dynamics*. Cambridge, U.K.: Cambridge Univ. Press, 1989.
- [27] G. L. Oppo and A. Politi, "Toda potential in laser equations," *J. Phys. B—Condensed Matter*, vol. 59, pp. 111–115, 1985.
- [28] E. Doedel, T. Fairgrieve, B. Sandstebe, A. Champneys, Yu. Kutznetsov, and S. Wang. AUTO97: Continuation and bifurcation software for ordinary differential equations. [Online]. Available: <http://indy.cs.concordia.ca/auto/main.html>.
- [29] J. R. Tredicce, N. B. Abraham, G. P. Puccioni, and F. T. Arecchi, "On chaos in lasers with modulated parameters: A comparative analysis," *Opt. Commun.*, vol. 55, p. 131, 1985.
- [30] Y. M. Yang and H. F. Liu, "Control of period doubling in modulated semiconductor lasers and its application to all-optical clock division," in *Proc. Photonic West 2001*, San José, CA, Paper 4283-47.
- [31] H. Lamela, G. Carpintero, and P. Acebo, "Truncation of the Feigenbaum sequence in directly modulated semiconductor lasers," *IEEE J. Quantum Electron.*, vol. 34, pp. 491–496, 1998.
- [32] H. Lamela, G. Carpintero, and F. Mancebo, "Period tripling and chaos in the dynamic behavior of directly modulated diode lasers," *IEEE J. Quantum Electron.*, vol. 34, pp. 1797–1801, 1998.
- [33] P. Colet, C. R. Mirasso, and M. San Miguel, "Memory diagram of single-mode semiconductor lasers," *IEEE J. Quantum Electron.*, vol. 29, pp. 1624–1630, 1993.



**Catalina Mayol** was born in Mallorca, Spain, in 1973. She is currently working toward the Ph.D. degree in physics at the University of the Balearic Islands (UIB), Palma de Mallorca, Spain.

She has worked in Lunds Tekniska Hogskola, Lund, Sweden, and Universidad de Cantabria, Santander, Spain. Her research includes applications of nonlinear dynamics to laser systems.



**Raúl Toral** was born in Barcelona, Spain, in 1958. He received the Ph.D. degree in physics from the Universidad de Barcelona, Barcelona, Spain, in 1985.

He is a Full Professor at the Physics Department, Universitat de les Illes Balears (UIB), Palma de Mallorca, Spain, and a Member of the Instituto Mediterráneo de Estudios Avanzados (IMEDEA, CSIC-UIB), Palma de Mallorca, Spain. He has participated in several European and Spanish projects. His research interests include Monte Carlo methods, kinetics of first-order phase transitions, pattern formation, stochastic resonance and noise-induced phase transitions, chaos and synchronization of chaotic systems, and applications of nonlinear dynamics.



**Claudio R. Mirasso** was born in Buenos Aires, Argentina, in 1960. He received the Ph.D. degree in physics from Universidad Nacional de la Plata, Argentina, in 1989.

He is an Associate Professor at the Physics Department of the Universitat de les Illes Balears, Palma de Mallorca, Spain. He has participated in several European and Spanish projects related to semiconductor laser dynamics and applications. His research interests include instabilities in semiconductor lasers, synchronization and control of chaotic semiconductor lasers, VCSELs, analog simulations, and applications of nonlinear dynamics to different systems.



**Sergei I. Turovets** was born in Ladec, Belarus, in 1961. He received the Diploma in physics from Moscow State University, Moscow, Russia, in 1983, and the Ph.D. degree in laser physics from the Institute of Physics, Academy of Sciences, Minsk, Belarus, in 1992.

From 1984 to 1999, he was with the Institute of Physics, Academy of Sciences of Belarus, where he was engaged in research on nonlinear dynamics in lasers. In 2000, he joined Siros Technologies, Inc., San Jose, CA. His current research interests include photonic CAD and semiconductor laser design.

Dr. Turovets is a recipient of Fellowship Awards from both the Royal Society, London, U.K., and the Ministry of Education and Culture, Madrid, Spain. He is a member of the IEEE Lasers and Electro-Optics Society.



**Luis Pesquera** is a Full Professor at the Modern Physics Department, Universidad de Cantabria, Santander, Spain, and Director of the Instituto de Física de Cantabria (Santander, Spain). He has participated in several European and Spanish projects. His research interests include laser diodes for optical communication systems, synchronization and control of chaotic laser diodes, VCSELs, semiconductor optical amplifiers, and soliton transmission.